Accepted Manuscript

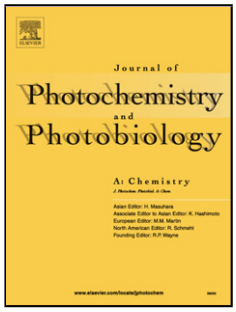

Title: $\{Ru(CO)_x\}$-core terpyridine complexes: lysozyme binding affinity, DNA and photoinduced carbon monoxide releasing properties

Authors: Ahmed M. Mansour, Ola R. Shehab

PII: S1010-6030(18)30511-2
DOI: https://doi.org/10.1016/j.jphotochem.2018.06.026
Reference: JPC 11343

To appear in: *Journal of Photochemistry and Photobiology A: Chemistry*

Received date: 18-4-2018
Revised date: 2-6-2018
Accepted date: 9-6-2018

Please cite this article as: Mansour AM, Shehab OR, $\{Ru(CO)_x\}$-core terpyridine complexes: lysozyme binding affinity, DNA and photoinduced carbon monoxide releasing properties, *Journal of Photochemistry and Photobiology, A: Chemistry* (2018), https://doi.org/10.1016/j.jphotochem.2018.06.026

This is a PDF file of an unedited manuscript that has been accepted for publication. As a service to our customers we are providing this early version of the manuscript. The manuscript will undergo copyediting, typesetting, and review of the resulting proof before it is published in its final form. Please note that during the production process errors may be discovered which could affect the content, and all legal disclaimers that apply to the journal pertain.

ACCEPTED MANUSCRIPT

{Ru(CO)$_x$}-core terpyridine complexes: lysozyme binding affinity, DNA and photoinduced carbon monoxide releasing properties

Ahmed M. Mansour, [a,b*] and **Ola R Shehab** [a]

[a] Department of Chemistry, Faculty of Science, Cairo University, Gamma Street, Giza, Cairo 12613, Egypt

[b] Institut für Anorganische Chemie, Julius-Maximilians-Universität Würzburg, Am Hubland, D-97074 Würzburg, Germany

* mansour@sci.cu.edu.eg;
ahmed.mansour@uni-wuerzburg.de

* Corresponding author

Graphical abstract

ACCEPTED MANUSCRIPT

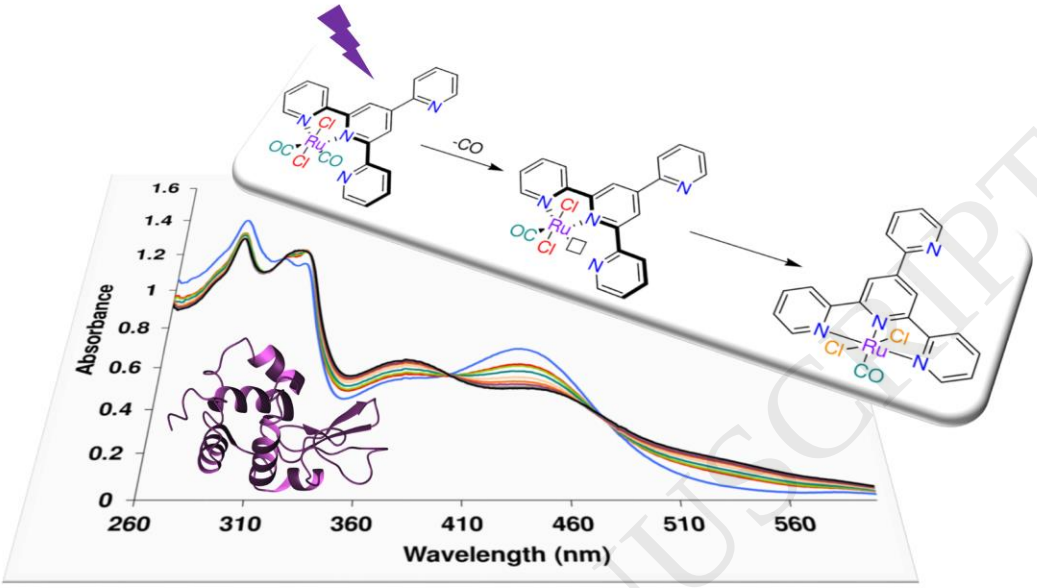

Highlights

- Stable protein adduct are formed in the dark and release CO upon illumination.
- Change of the coordination mode upon the release of the CO molecule.
- Properties of the photo induced CO release at 365 nm.
- TD-DFT data compares well with the experimental data.

Abstract

Reaction of 4'-(2-pyridyl)-2,2':6',2''-terpyridine (L^{PY}) and 4'-(4-phenylmorpholine)-2,2':6',2''-terpyridine (L^{morph}) with $\{[RuCl_2(CO)_3]\}_2$ in methanol afforded $[RuCl_2(L^{PY}\text{-}\kappa^2N^1N^2)(CO)_2]$ (**1**) and a mixture of $[RuCl_2(L^{moph}\text{-}\kappa^2N^1N^2)(CO)_2]$/$[RuCl_2(L^{morph}\text{-}\kappa^3N^1N^2N^3)(CO)]$ (**2**), respectively. Their photoactivatable CO releasing properties are investigated upon the exposure to light source at 365 nm. One CO molecule is released from **1** at the excitation wavelength 365 nm, while the ligand changes its bidentate mode into the meridional tridentate one. The illumination profile and the influence of the uncoordinated pyridine arm on CO release

ACCEPTED MANUSCRIPT

were examined by solution ^{1}H and ^{13}C NMR studies. The electronic transitions are studied by TDDFT. The DNA and hen white egg lysozyme binding affinity of the complexes are studied by UV/Vis. and electrospray ionization mass spectrometry. Stable lysozyme complexes, capable of photo induce CO, are formed *via* the loss of the labile chloride ligands or terpyridine moiety.

Keywords:

Photoinduced; lysozyme; Ruthenium dicarbonyl; TDDFT

Introduction

The problem of lack of the target specificity of carbon monoxide gas [1], administrated for the anti-inflammatory, anti-proliferative and signaling properties, encouraged the researchers to initiate new ways by which CO could be supplied in a controlled way without delivering toxic quantities to the whole body. *Carbon monoxide releasing molecules* (CORMs) that are enzymatically triggered [2] or liberate certain amount of CO upon the change of the redox state [3], pH value [4], thermal heating [5] and light exposure [6], have been introduced as an alternative way to the inhalation system. Organometallic classes (e.g. Borano carboxylates [7], silacarboxylates [8] and metal carbonyls [6]) and organic compounds such as α,α-dialkylaldehydes [9] and oxalates [10] have been studied in the context of CORMs. The term photoCORM has been defined by Ford and his coworkers to categorize a group of CORMs capable of release CO upon the illumination [11], although two simple metal carbonyls [$Mn_2(CO)_{10}$] (CORM-1) and $Fe(CO)_5$ have been early investigated as CO releasers [12]. Next, the CO releasing properties of ([Ru(Glycinate)$(CO)_3Cl$]) (CORM-3) [13] have been investigated; when dissolved in water, one CO molecule is immediately liberated.

Few examples of Ru(II) carbonyl complexes [14-19] have been investigated as CORMs though they exhibit interesting anti-inflammatory properties [20]. The CO releasing properties of [Ru(qmtpm)(CO)Cl(PPh_3)]BF_4 upon the exposure to the low power (15 mW/cm^2) visible light have been studied by Mascharak group [17]. Only one CO equivalent was released from [$RuCl_2$(N-N)$(CO)_2$] (N-N = anti-anxiety drug, Bromazepam)

ACCEPTED MANUSCRIPT

[15] as quantitatively estimated with the myoglobin assay. Ruthenium(II) carbonyl complexes of 2,2´:6´,2´´-terpyridine (tpy) have been studied as photo and electrocatalyst for the reduction of CO_2 [21]. One CO molecule is liberated from κ^3N^1,N^2,N^3-terpyridine Ru(II) dicarbonyl complex at 365 nm [14]. The change of the bidentate mode of terpyridine and closely related 2,6-bis-(benzimidazol-2´-yl) pyridine derivatives into the tridentate manner is a subject of interest [18, 21]. Alkylation of 2,6-bis-(benzimidazol-2´-yl) pyridine prior to reaction with $\{[RuCl_2(CO)_3]\}_2$ (CORM-2) gave rise to blue-light induced Ru(II) photoCORM capable of release CO upon the exposure to light at 468 nm [18]. Treatment of $[RuX_2(CO)_2(\kappa^2N^1N^2\text{-tpy})]$ (X = Cl and Br) with trimethylamine N-oxide afforded the monocarbonyl terpyridine Ru(II) complexes, $[RuX_2(CO)(\kappa^3N^1N^2N^3\text{-tpy})]$ (tpy = 2,2':6',2''-terpyridine) as established by X-ray crystallography [22].

The interactions between some model proteins (e.g. hen egg white lysozyme (HEWL) and human carbonic anhydrase II) and Ru(II) carbonyl complexes; CORM-2 [23], CORM-3 [24], $[Ru(CO)_3Cl_2(1,3\text{-thiazole})]$ [25], $[Ru(CO)_3Cl_2(Imidazole)]$ [26], and $[Ru(CO)_2Cl_2(2\text{-}(2\text{-(pyridyl)benzimidazole})]$ [18, 19]) have been reported. Such interactions affect the pharmacological profile and drug-delivery. An interesting review about the protein affinity of some Ru(II) complexes has been recently introduced by Merlino [27]. CORM-3 is mainly bound to lysozyme, in the form of ($[Ru(CO)_2(H_2O)_3]^{2+}$), at His15 side chain as early investigated by Romao and coworkers [24]. The crystal structure of lysozyme/$[Ru(CO)_3Cl_2(Imidazole)]$ adduct [26] reveals that the interaction site is the His15 side chain. Non-covalent interaction modes of HEWL have been observed by some Ru(II) photoCORMs bearing bidentate benzimidazole ligands [18, 19].

To find new motivating photochemical and photophysical properties close to that reported by the parent terpyridine and 2,6-bis-(benzimidazol-2´-yl) pyridine photoCORMs, new $\{Ru(CO)_x\}$-terpyridine complexes, (Scheme 1) capable of release CO upon the exposure to light source, are synthesized. To understand the electronic transitions, TDDFT calculations are performed. The illumination profiles are examined by solution NMR studies to inspect if the chelation mode is changing or preserving during the liberation of CO molecule or not. The interaction between the complexes and DNA or HEWL have been studied by UV/Vis. and electrospray ionization mass spectrometry, respectively.

Results and discussion

Synthesis and characterization

The terpyridine ligands (L^{PY} and L^{morph}) (Scheme 1) are synthesized in one simple step *via* the condensation of 2-acetylpyridine with the corresponding aldehyde [28] and characterized by elemental analysis, ESI-MS, IR and NMR spectroscopies (Fig. S1-3). Reaction of 4'-(2-pyridyl)-2,2':6',2''-terpyridine (L^{PY}) and 4'-(4-

ACCEPTED MANUSCRIPT

phenylmorpholine)-2,2':6',2''-terpyridine (L^{morph}) with $\{[RuCl_2(CO)_3]\}_2$ in methanol afforded $[RuCl_2(L^{PY}$-$\kappa^2N^1N^2)(CO)_2]$ (**1**) and a mixture of $[RuCl_2(L^{moph}$-$\kappa^2N^1N^2)(CO)_2]$/$[RuCl_2(L^{morph}$-$\kappa^3N^1N^2N^3)(CO)]$ (**2**), respectively. The structures are elucidated by different analytical and spectral methods (Fig. S4-6). The AT IR spectrum of **1** shows two stretches at 2070 and 2019 cm^{-1} corresponding to the symmetrical and anti-symmetrical stretching modes of two CO molecules. It is not easy to allocate the ν(C-Cl) modes in the far-IR range to get some information about the geometrical stereochemistry of **1**. However, the difference between the wavenumbers of the CO stretching modes is used to suggest which isomer is present in the solid state [18, 19]. The value of Δν(CO) of **1** is 51 cm^{-1}, which compares well with the presence of the CO ligands in the *cis*-positions as established with most of the previously published crystal data of *cis*-$[Ru(CO)_2Cl_2L]$ complexes bearing bidentate ligands. The ESI-MS of **1**, in the positive mode, shows two peaks at *m/z* = 502.9829 and 441.0275 due to $[RuCl(CO)_2L^{PY}]^+$ and $[Ru(CO)L^{PY}]^+$ in that order. The ^{1}H NMR spectrum of **1** consists of nine aromatic signals arising from the absence of the C2 axis of symmetry and coordination of terpyridine ligands to Ru(II) ion *via* κ^2N^1,N^2 bidentate mode. In the ^{13}C NMR spectrum of **1** (Fig. S4), two ^{13}CO signals are observed at 194.1 and 187.0 ppm characteristic of the dicarbonyl Ru(II) complex.

The IR spectrum of **2** displays a very strong band at 1946 cm^{-1} as well as two medium bands at 2061 and 2003 cm^{-1}. The vibrational pattern of the CO modes does not match with the presence of *fac*-$Ru(CO)_3$ moiety [13]. The band at 1946 cm^{-1} could be assigned to ν(CO) in $[RuCl_2(L^{morph}$-$\kappa^3N^1N^2N^3)(CO)]$ that agrees with the published data of *cis*-$[RuX_2(CO)(\kappa^3N^1N^2N^3$-tpy)] (X = Cl, 1948 cm^{-1} and X = Br, 1944 cm^{-1}) [22]. The other bands at 2061 and 2003 cm^{-1} may be allocated to ν^s(CO) and ν^{as}(CO) of cis-$[RuCl_2(L^{moph}$-$\kappa^2N^1N^2)(CO)_2]$ with Δν(CO) of 58 cm^{-1}. Partition decarbonylation of $[RuCl_2(L^{moph}$-$\kappa^2N^1N^2)(CO)_2]$, during the reaction time, affords $[RuCl_2(L^{morph}$-$\kappa^3N^1N^2N^3)(CO)]$, while the L^{morph} changes its bidentate mode into the tridentate one. Decarbonylation can be achieved *via* thermal, electrochemical and photochemical process [29]. For example, heating of tricarbonyl Mn(I) terpyridine complexes in acetonitrile leads to formation of a mixture of tricarbonyl and dicarbonyl species [29]. Other evidences of the presence of a mixture of mono- and dicarbonyl species are gained from TLC (1:1 (v/v) CH_3Cl/MeOH; R_f = 0.65 and 0.81) and other spectroscopic tools. The positive mode ESI-MS of **2**, in methanol, shows two unique fragments; $[Ru(OCH_3)(CO)_2L^{morph}]^+$ (m/z = 583.0904) and $[RuCl(CO)L^{morph}]^+$ (m/z = 559.0459). The ^{13}C NMR spectrum of **2** is characterized by three ^{13}CO signals at δ = 193.6, 191.6 and 186.8 ppm. The signals at δ = 193.6 and 186.8 ppm compare well with that observed in **1** for the dicarbonyl species, while that at δ = 191.6 ppm may be allocated to ^{13}CO in $[RuCl_2(L^{morph}$-$\kappa^3N^1N^2N^3)(CO)]$.

Light triggered CO release properties

ACCEPTED MANUSCRIPT

Two electronic absorption bands are observed at 294 and 334 nm in the DMSO solution of **1** (Fig. 1a). The calculated spectrum of *cis*-(CO,CO)-[$RuCl_2(L^{PY}$-$\kappa^2N^1N^2)(CO)_2$] (**1**), at TD/cam-B3LYP/LANL2DZ level of theory , is characterized by three transitions at 267, 293 and 407 nm due to HOMO-3→LUMO, HOMO-2→LUMO and HOMO→LUMO+2, respectively. The electronic transition at 407 nm has ground- and excited states composed of d(Ru) character forming d-d transition. In general, the ground-state of the octahedral Ru(II) complexes is $^1A_{1g}$ and thus the calculated singlet-singlet transition at 407 nm may be assigned to $^1A_{1g}\rightarrow{}^1T_{1g}$ [30]. HOMO-2, which is 0.14 eV lower than HOMO, has a character of d(Ru)/π(L^{PY}), while LUMO is contained upon the ligand system (Fig. 2a). Accordingly, the transition at 293 nm is MLCT from the filled t_{2g} to ligand π^* molecular system. Experimentally, the aerated solution of **1** is stable for 14 h (Fig. S7). Illumination of **1** at 365 nm, using a 6 UV hand lamp, results in grownup of a broad band at 430 nm and blue-shift of the native bands to 290 and 327 nm. The photochemical process has been assigned with the aid of the myoglobin assay [31]. Although, the assay has few drawbacks such as the interference from the highly colored compounds, turbidity and dependent of the CO photogenerated upon the quantity of the dithionate used as a reducing agent [32], it is still a simple assay to explore the CO release. The kinetics of the CO release, under these reduced conditions, are slow and illumination of 10 µM of **1** leads to formation of only 6.9 µM MbCO (Fig. S8). The rate constant is (1.3 ±0.1) × 10^{-3} s^{-1} and the $t_{1/2}$ is 8.87 ± 0.2 min.

The electronic spectrum (Fig. 1b) of **2** displays five transitions at 293, 315, 328, 381 and 442 nm. The TD/cam-B3LYP/LANL2DZ spectrum of *cis*-(CO,CO)-[$RuCl_2(L^{morph}$-$\kappa^2N^1N^2)(CO)_2$] is characterized by three electronic transitions at 253, 282 and 408 nm arising from the transitions of HOMO-2→LUMO+1, HOMO-3→LUMO and HOMO-1→LUMO+2, respectively. The descriptions and energies (eV) of the frontier molecular orbitals involved in the main transitions of *cis*-(CO,CO)-[$RuCl_2(L^{morph}$-$\kappa^2N^1N^2)(CO)_2$] are given in Fig. 2b. The calculated band at 408 nm is allocated for d-d transition, where the transition takes place from the lower lying d-orbitals to the empty d_{z^2} orbital. The transitions at 253 and 282 nm are assigned to π-π^*/MLCT. On the other hand, the two geometrical isomers of [$RuCl_2(L^{morph}$-$\kappa^3N^1N^2N^3)(CO)$], the other component of the mixture **2**, were optimized and their electronic transitions were calculated. Trans-(Cl,Cl) [$RuCl_2(L^{morph}$-$\kappa^3N^1N^2N^3)(CO)$] (-1497.214108 Hartree) is more stable than the cis-isomer (-1497.210154 Hartree). As shown in Fig. 2C, the lowest energy transition (406 nm) of the trans-isomer, assigned to MLCT/d-d, is red shifted with respect to the cis-isomer (388 nm). Experimentally, the aerated DMSO solution of **2** is stable in the dark for 14 h (Fig. S9). Two isosbestic points are observed at 480 and 405 nm during the illumination of the pre-incubated solution of **2** (Fig. 1b). Compared with **1**, the rate ((1.0 ±0.1) × 10^{-3} s^{-1} and $t_{1/2}$ is 10.74 ± 0.1 min) and quantity (0.3 CO equivalents) of the CO photogenerated from a sample of 10 µM of **2** are slower and lower. This could be also taken as an evidence that the monocarbonyl

ACCEPTED MANUSCRIPT

species constitutes the major component in the reaction mixture of **2** as the number of CO equivalents exposed to the light source is lower than in **1** at the same concentration. In comparison, the presence of free pyridine arm close to the coordination sphere in **1** facilitates the release of one CO *via* the occupation of the empty position of the octahedral geometry, prior to loss of one CO, and so the releasing kinetics are faster [18].

The photolysis profiles of the complexes are examined by solution ^{1}H and ^{13}C NMR studies. As shown in Fig. 3, the typical signals of the terpyridine bidentate mode disappear during the illumination of the [D_6] DMSO solution of **1** at 365 nm and a new set of signals assigned to the meridional tridentate mode grows with time. A set of two doublets and two triplets characteristic of binding the closely uncoordinated pyridine ring are observed at δ = 9.08, 9.01, 8.34 and 7.78 ppm. Analysis of the ^{13}C NMR spectrum (Fig. 4) of the illuminated solution reveals that only CO molecule is observed at δ = 198.8 ppm. Therefore, the terpyridine ligand changes its coordination mode during the illumination and only one CO molecule is released that compares well with the myoglobin assay. The ^{1}H NMR spectral changes of **2**, in $CDCl_3$, upon the illumination are given in the supporting information, Fig. S10. No significant change, comparable to that observed in **1**, is monitored, which reflects again that [$RuCl_2(L^{morph}$-$\kappa^3N^1N^2N^3)$(CO)] is the major constituent of **2** and consequently the meridional tridentate mode is preserving during the illumination period.

DNA binding studies

The interaction between DNA and the drugs offers some information about replication, transcription and the mutation of the genes. This may be achieved *via* the covalent and non-covalent modes. Exchange of the chloride ligands in cisplatin with the nitrogen bases is a covalent interaction. Intercalation, groove (major and minor) and electrostatic modes are the noncovalent interactions. Here, the DNA binding affinity of the investigated photoCORMs is spectrophotometrically studied. The change of the position and/or intensity of the bands as well as the grownup of new bands upon the addition of Calf-thymus DNA to the CORM solution are monitored and compared with the UV/Vis. photolysis profiles (Fig. 1). The titration plots of **1** and **2** are shown in Fig. 5. A new shoulder grows up in the range of 400-500, two isosbestic points are observed at 302 and 357 nm as well as the intensity of the band at 334 nm decreases during the titration period of **1**. The DNA plot of **1** compares well with the illumination profile (Fig. 1a), which suggests that CT DNA may be covalently interact with **1** *via* the loss of one CO molecule. As shown in Fig. 5b, addition of DNA to a solution of **2** leads to hyperchromic effect [33], which may indicate the dual nature of covalent and non-covalent intercalative interactions [34]. However, in the absence of crystal structure, it is difficult

ACCEPTED MANUSCRIPT

to confirm the type of interaction either covalent or noncovalent between DNA and the investigated complexes.

Interaction with lysozyme

Subsequent the administration of the biologically active compounds, there is a highly affinity to binding to the histidyl proteins. Such interactions could influence the drug delivery and the pharmacological profile. Alternatively, some proteins such as hen egg white lysozyme (HEWL) has been used as a biocompatible carrier of some CORMs to deliver carbon monoxide into the living cells [35]. HEWL accommodates CORMs mainly at His15 side chain [36], and minorly at Asp18 and Asp52. HEWL has been used as a perfect model because of its small size and positively charged groups that is appropriate for the measurements of the electrospray ionization mass spectrometry. In the present contribution, the lysozyme affinity of **1** and **2** is studied in the solution at the room temperature, in a ratio of 1:5 (complex:HEWL), by the positive mode ESI-MS (Fig. 6). In the dark, complex **1** reacts with HEWL to give an adduct peak at m/z = 1646.4223 Da (z = 9, $[RuCl(L^{PY})(CO)_2]^+$). Four adducts containing the following species, $\{Ru^{II}\}$ (m/z = 1601.0975), $\{Ru^{II}(CO)_2Cl\}^+$ (m/z = 1611.9833), $\{[RuClL^{PY}]^+\}$ (m/z = 1639.9848) and $\{[RuCl_2(CO)L^{PY}]\}$ (m/z = 1647.3174) are observed upon the illumination of the reaction mixture at 365 nm for 20 min. When product **2** interacts with HEWL, two adduct peaks of $\{[RuCl_2(CO)L^{morph}]\}$ are observed corresponding to bind of one (m/z = 1656.6503) and two species (m/z = 1722.2102). Three adduct comprising the next species, $\{Ru^{II}\}$ (m/z = 1601.4312), $\{Ru^{II}(CO)_2Cl\}^+$ (m/z = 1611.8741) and $\{[RuCl_2(CO)L^{morph}]\}$ (m/z = 1656.6586) are detected upon the exposure of the mixture to source light for 20 min. Therefore, bioconjugation of HEWL with the studied photoCORM leads to stable adducts capable of release CO upon the exposure to light source.

Conclusion

In summary, more conjugated terpyridine ligand system has been utilized in the synthesis of $\{Ru(CO)_x\}$-core complexes capable of release carbon monoxide upon the exposure to light source at 365 nm. The photolysis profiles have been investigated by UV/Vis. and NMR spectroscopies. The terpyridine ligand changes the bidentate coordination mode into the meridional, tridentate manner during the illumination. The myoglobin assay and ^{13}C NMR studies confirms the release of one CO molecule. Time-dependent density functional calculations have been used to understand the electronic transitions observed by the complexes. In the dark, the reactivity of the complexes towards DNA has been spectrophotometrically studied. Interestingly, the DNA-complex plot resembles the illuminated profile that may reflect an interaction *via* the loss of CO molecule(s). The lysozyme binding affinity of the complexes is investigated by means of the electrospray mass spectrometry in the dark and upon the exposure to light. Stable protein

ACCEPTED MANUSCRIPT

adduct peaks are observed, which can be easily photo triggered. Therefore, lysozyme could be used as biocompatible carrier of this class of photoCORMs to deliver CO into the living cells.

Experimental section

Materials and instruments

Degassed methanol and argon atmosphere are used in the synthesis of the terpyridine derivatives and the Ru(II) dicarbonyl complexes. [{$RuCl_2(CO)_3$}$_2$] was purchased from Strem Chemicals. ^{1}H and ^{13}C NMR spectra are recorded with Brucker-Avance 500 (^{1}H, 500.13 MHz; ^{13}C{^{1}H}, 125.77 MHz) and Brucker-Avance 400 (^{1}H, 400.40 MHz; ^{13}C{^{1}H}, 100.70 MHz) spectrometers. Assignments are done with aid of the two-dimensional NMR; {^{1}H, ^{1}H} COS90 and {^{1}H, ^{13}C} HSQC. Electrospray mass spectra are run with a ThermoFisher Exactive Plus instrument with an Orbitrap mass analyzer at a resolution of R = 70.000 and a solvent flow rate of 5 µL min. UV/Vis. spectra are recorded on an Agilent 8453 diode array spectrophotometer. Elemental micro-analysis is carried out with a Vario Micro Cube analyzer of Elementar Analysensysteme or an EA 3000 elemental analyzer from HEKtech. IR spectra are recorded in the solid state on a Nicolet 380 FT-IR spectrometer equipped with a smart iFTR accessory.

Synthesis of 2,2′:6′,2″ terpyridine ligands

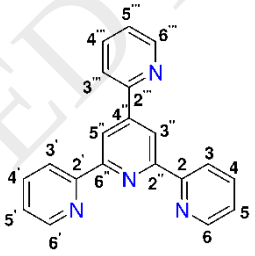

L^{PY} [37]: 10 mmol of 2-acetylpyridine (1.21 g) is added to ammonia solution (20 mL) containing 2 g of potassium tert-butoxide and 20 mL ethanol. 5 mmol of 2-pyridine carboxaldehyde (0.55 g) is transferred to the reaction flask, where a dark brown color is immediately developed. The reaction mixture is stirred at room temperature for 20 h. The brown color diminishes with time, and a white precipitate is formed. The precipitate is collected by filtration and washed several times with water. Recrystallization was performed from DMSO. Yield: 49 % (0.75 g, 2.41 mmol). IR (ATR): $\breve{\upsilon}$ = 3057 (m, CH), 3014 (w, CH), 1602 (w, CN/CC), 1580, 1546, 1465, 1432, 1389, 1262, 1069, 990, 775, 729. ^{1}H NMR ($CDCl_3$, 400.40 MHz): δ = 9.11 (s, 2H, H3′′/5′′), 8.79 (m, 1H, H6′′′), 8.74 (m, 2H, H6/H6′), 8.65 (m, 2H, H3/H3′), 8.07 (d, $J_{H,H}$ = 7.9, 1H, H3′′′), 7.87-7.82 (m, 3H, H4/H4′/H4′′′), 7.33 (m, 3H, H5/H5′/H5′′′) ppm. ^{13}C NMR ($CDCl_3$, 100.68 MHz): δ = 156.1

ACCEPTED MANUSCRIPT

(C2'''), (156.02, 156.00) (C2/C2'), 155.00 (C4''),150.01 (C6'''), (149.04, 149.02) (C6/C6'), (148.69, 148.67) (C2''/C6''), (137.02, 136.98, 136.86) (C4/C4'/C4'''), (123.87, 123.85, 123.73) (C5/C5'/C5'''), 121.40 (C3'''), (121.30, 121.29) (C3/C3'), 118.73 (C3''), 118.70 (C5'') ppm. $C_{20}H_{14}N_4$: C 77.40, H 4.55, N 18.05, found C 77.34, H 4.65, N 18.36.

L^{morph}: The new terpyridine derivative is synthesized following the same procedure as L^{PY} except that 4-(4-morpholinyl)benzaldehyde (0.95 g) is used. The yellowish-white precipitate is recrystallized from ethanol. Yield: 65 % (1.29 g, 3.0 mmol). IR (ATR, diamond): $\breve{\upsilon}$ = 3059 (w, CH), 2969 (w, CH), 2837 (w, CH), 1611 (m, CC/CN), 1576, 1516, 1467, 1384, 1220, 1118, 1033, 925, 781, 726. ^{1}H NMR ($CDCl_3$, 500.13 MHz): δ = 8.66 (m, 2H), 8.64 (s, 2H), 8.59 (d, $J_{H,H}$ = 8.0 Hz, 2H), 7.80 (m, 4H), 7.27 (m, 2H), 6.94 (d, $J_{H,H}$ = 8.9 Hz, 2H), 3.82 (m, 4H), 3.19 (m, 4H) ppm. ^{13}C-NMR ($CDCl_3$, 125.75 MHz): δ = 156.5, 155.8, 151.8, 149.7, 149.0, 136.9, 129.1, 128.1, 123.7, 121.4, 117.9, 115.3, 66.9, 48.7 ppm. ESI-MS (positive mode, acetone): *m/z* = 395.1864 $[M+H]^+$. $C_{25}H_{22}N_4O$: C 76.12, H 5.62, N 14.20, found, C 76.19, H 5.61, N 14.37.

Synthesis of complexes:

0.34 mmol of the terpyridine ligand (L^{PY}, 105 mg and L^{morph}, 134 mg) is added to 25 mL methanolic solution of $[Ru(CO)_3Cl_2(MeOH)]$, formed by heating 87 mg of $[Ru(CO)_3Cl_2]_2$ (0.17 mmol) in methanol for 3 h. The reaction mixtures are heated to reflux overnight (16 h), while the solution is protected from the light. Complex **1** is precipitated as a violet powder by adding diethyl ether, while mixture **2** is precipitated as a red powder from the reaction. The precipitates are collected, washed with diethyl ether, and dried *in vacuo* for few days.

$[RuCl_2(L^{PY}\text{-}\kappa^2N^1N^2)(CO)_2]$ (**1**): Color: violet powder. Yield: 52 % (95 mg, 0.176 mmol). IR (ATR, diamond): $\breve{\upsilon}$ = 3033 (w, CH), 2070 (vs, C≡O), 2019 (vs, C≡O), 1605, 1475, 1413, 1248, 780. ^{1}H NMR ([D_6]DMSO, 500.13 MHz): δ = 9.49 (s, 2H), 9.12 (d, $J_{H,H}$ = 7.9 Hz, 2H), 8.97 (dd, $J_{H,H}$ = 5.5 Hz, $J_{H,H}$ = 1.0 Hz, 2H), 8.94 (dd, $J_{H,H}$ = 4.7 Hz, $J_{H,H}$ = 1.1 Hz, 1H), 8.70 (d, $J_{H,H}$ = 7.9 Hz, 1H), 8.43 (td, $J_{H,H}$ = 7.8 Hz, $J_{H,H}$ = 1.3 Hz, 2H), 8.21 (td, $J_{H,H}$ = 7.5 Hz, $J_{H,H}$ = 1.8 Hz, 1H), 7.85 (m, 2H), 7.71 (m, 1H). ^{13}C-NMR ([D_6]DMSO, 125.75 MHz): δ = 194.1 (C≡O), 187.0 (C≡O), 157.3, 156.7, 154.5, 152.9, 151.6, 151.4, 150.3, 140.9, 138.9, 138.1, 129.0, 127.7, 126.1, 126.0, 124.6, 123.1, 121.4, 120.2, 119.6. ESI-MS (positive mode, methanol): *m/z* = 502.9829 $[RuCl(CO)_2L^{PY}]^+$, 441.0275 $[RuCl(CO)L^{PY}]^{2+}$. $C_{22}H_{14}Cl_2N_4O_2Ru.H_2O$: C 47.49, H 2.90, N 10.07, found C 47.76, H 3.21, N 10.20.

$[RuCl_2(L^{moph}\text{-}\kappa^2N^1N^2)(CO)_2]$/$[RuCl_2(L^{morph}\text{-}\kappa^3N^1N^2N^3)(CO)]$ (**2**): Color: red powder. Yield: 56 % (118 mg, 0.189 mmol). IR (ATR, diamond): $\breve{\upsilon}$ = 3067 (w, CH), 2836 (w, CH), 2061 (m, C≡O), 2003 (m, C≡O), 1948 (vs, C≡O), 1591, 1528, 1413, 1216, 1119, 928, 786. ^{1}H NMR ($CDCl_3$, 500.13 MHz): δ = 9.49 (s, 1H), 9.17 (m, 2H), 8.52

ACCEPTED MANUSCRIPT

(m, 2H), 8.18 (m, 3H), 7.80 (m, 2H), 7.50 (m, 2H), 6.98 (m, 2H), 3.87 (m, 4H), 3.29 (m, 4H). ^{13}C-NMR ($CDCl_3$, 125.75 MHz): δ = 193.6 (C≡O), 191.6 (C≡O), 186.8 (C≡O), 186.8 (C≡O), 158.4, 157.9, 157.8, 157.2, 155.7, 154.6, 154.3, 153.9, 153.5, 153.4, 153.2, 152.8, 150.7, 149.0, 141.4, 137.9, 130.7, 128.8, 128.4, 128.0, 127.1, 125.1, 123.6, 123.4, 121.1, 119.6, 118.9, 115.2, 114.7, 66.8, 66.7, 47.9, 47.4. ESI-MS (positive mode, methanol): *m/z* = 583.0904 $[Ru(OCH_3)(CO)_2L^{morph}]^+$, 559.0459 ($[RuCl(CO)L^{morph}]^+$). $C_{53}H_{44}Cl_4N_8O_5Ru_2.3H_2O$ (1:1 mixture): C 50.09, H 3.97, N 8.82, found C 50.23, H 3.96, N 8.87.

Density functional theory calculations

Ground-state geometry optimization of the complexes, in the singlet-state, have been performed using Becke-3-parameter (exchange) Lee–Yang–Parr (B3LYP) functional [38] and the effective core potential (ECP) of the Hady and Wadt, LANL2DZ basis set [39]. The geometry has been checked as a local minimum *via* the calculation of the vibrational modes. The time-dependent DFT spectra have been calculated using the hybrid exchange-correlation functional CAM-B3LYP [40], with a long-range correction term, and LANL2DZ basis set using the default polarizable continuum model. The calculations have been done with Gaussian 03 package [41].

DNA binding studies

The DNA binding affinity towards the ruthenium dicarbonyl complexes is spectrophotometrically studied at the room temperature. Calf-thymus DNA is dissolved in Tris-HCl buffer (pH = 7.4, 5 mM tris(hydroxymethyl) amino methane, 50 mM NaCl) and the concentration is adjusted by recording the absorbance values at 260 (ε_{260} = 6600 $Lmol^{-1}cm^{-1}$) [42] and 280 nm. The A_{260}/A_{280} is 1.9 that reveals that the DNA is suitably free of protein. The UV/Vis absorption titration is performed by placed a certain amount of the complex (dissolved in DMSO) in the cuvette and gradually the concentration of CT DNA is increased. Subsequent the addition of the DNA, the solutions (4 % DMSO/buffer) are agitated for 10 min. Then the electronic spectrum is recorded. The procedure is repeated until slightly change is observed.

Myoglobin assay

The number of CO equivalents released from the complexes upon the exposure to the UV/Vis hand lamp (365 nm, UVIlite LF-206LS, 6 W, UVItec Ltd, Cambridge, UK) have been determined by the myoglobin assay as previously reported [31]. Ferrioxalate actinometry assay has been done to determine the photo flow of the light source [14]. The sealed cuvette of the complex solution is positioned perpendicular to the light

ACCEPTED MANUSCRIPT

source at a distance of 3 cm. The UV/Vis spectra have been recorded on an Agilent 8543 diode array spectrophotometer until no more spectral changes have been observed. Dark stability measurements have been performed over 14 h.

Interaction with protein

The lysozyme binding affinity of the complexes has been studied by mixing a molar ratio of 1:5 lysozyme: complex and directly measured by orbital high-resolution mass spectrometer (ThermoFisher Exactive plus orbitrap) equipped with the conventional electrospray ionization source). The working conditions are as follows: spray voltage 3.80 KV, capillary voltage 45 V, and capillary temperature 320 ºC. For acquisition, Thermo Xaclibur qual is used.

Acknowledgments

Ahmed Mansour thanks the Alexander *von* Humboldt Foundation for Georg Forster postdoctoral fellowship. Prof. Dr. Ulrich Schatzschneider, Julius-Maximilians-Universität Würzburg, Germany is acknowledged for giving the author use of some of the analytical facilities of the institution.

References:

[1] R. Motterlini and L. E. Otterbein, *Nat. Rev. Drug Discovery*, 2010, **9**, 728; C. C. Romao, W. A. Blättler, J. D. Seixas and G. J. L. Bernardes, *Chem. Soc. Rev.*, 2012, **41**, 3571.

[2] E. Stamellou, D. Storz, S. Botov, E. Ntasis, J. Wedel, S. Sollazzo, B. K. Kraemer, W. Van-Son, M. Seelen, and H. G. Schmalz, *Redox Biol.*, 2014, **2**, 739.

[3] B. J. Aucott, J. S. Ward, S. G. Andrew, J. Milani, A. C. Whitwood, J. M. Lynam, A. Parkin, and I. J. S. Fairlamb, *Inorg. Chem.*, 2017, **56(9)**, 5431; F. Zobi, O. Blacque, R. A. Jacobs, M. C. Schaub and A. Yu. Bogdanova, *Dalton Trans.* 2012, **41**, 370.

[4] F. Zobi, A. Degonda, M. C. Schaub, and A. Y. Bogdanova, *Inorg. Chem.* 2010, **49**, 7313.

[5] P. C. Kunz, H. Meyer, J. Barthel, S. Sollazzo, A. M. Schmidt, and C. Janiak, *Chem. Commun.*, 2013, **49**, 4896.

[6] J. Niesel, A. Pinto, H. W. Peindy, K. N'Dongo, I. Merz, I. Ott, R. Gust, and U. Schatzschneider, *Chem. Commun.*, 2008, 1798; R. D. Rimmer, A. E. Pierri, and P. C. Ford, *Coord. Chem. Rev.* 2012, **256**, 1509; M. A. Gonzalez, and P. K. Masharak, *J. Inorg. Biochem.* 2014, **133**, 127; M. A. Wright and J. A. Wright, *Dalton Trans.* 2016, **45**, 6801; E. Kottelat and Z. Fabio, *Inorganics* 2017, **5(2)**, 24.

ACCEPTED MANUSCRIPT

[7] R. Motterlini, P. Sawle, J. Hammad, R. Alberto, R. Foresti, and C. J. Green, *FASEB J.*, 2004, **18**, 284.
[8] S. D. Friis, R. H. Taaning, A. T. Lindhardt, T. Skrydstrup, *J. Am. Chem. Soc.*, 2011, **133**, 18114.
[9] M. N. De Matos, and C. C. Romão, *US Pat., 2007219120A1*, 2007.
[10] P. Peng, C. Wang, Z. Shi, V. K. Johns, L. Ma, J. Oyer, A. Copik, R. Igarashi, and Y. Liao, *Org. Biomol. Chem.,* 2013, **11**, 6671; H. Yamada, N. Ono, K. Takahashi, T. Okujima, H. Uno, N. Uno, and S. Fukuzumi, *J. Mater. Chem.*, 2010, **20**, 3011.
[11] R. D. Rimmer, H. Richter, and P. C. Ford, *Inorg. Chem.* 2010, **49**, 1180.
[12] R. Motterlini, J. Clark, R. Foresti, P. Sarathchandra, B. Mann, and C. Green, *Circ. Res.* 2002, **90**, E17.
[13] T. R. Johnson, B. E. Mann, I. P. Teasdale, H. Adams, R. Foresti, C. J. Green, and R. Motterlini, *Dalton Trans.* 2007, 1500.
[14] C. Bischof, T. Joshi, A. Dimri, L. Spiccia, and U. Schatzschneider, *Inorg. Chem.* 2013, **52**, 9297.
[15] A. M. Mansour, *Appl. Organometal Chem.* 2017, **31**, e3564.
[16] S. J. Carrington, I. Chakraborty, J. R. Alvarado and P. K. Mascharak, *Inorg. Chim. Acta* 2013, 407, 121.
[17] I. Chakraborty, S. J. Carrington, and P. K. Mascharak, *Acc. Chem. Res.* 2014, **47**, 2603.
[18] A. M. Mansour and O. R. Shehab, *Eur. J. Inorg. Chem.* 2017, 4299.
[19] A. M. Mansour, *Eur. J. Inorg. Chem.* 2018, 852.
[20] W. Fukuda, T. Takagi, K. Katada, K. Mizushima, T. Okayama, N. Yoshida, K. Kamada, K. Uchiyama, T. Ishikawa, O. Handa, H. Konishi, N. Yagi, H. Ichikawa, T. Yoshikawa, G. Cepinskas, Y. Naito and Y. Itoh, *Dig. Dis. Sci.*, 2014, **59**, 1142; C. C. Romão, W. A. Blättler, J. D. Seixasab and G. J. L. Bernardes, *Chem. Soc. Rev.*, 2012, **41**, 3571; A. Yabluchanskiy, P. Sawle, S. Homer-Vanniasinkam, C. J. Green, R. Foresti and R. Motterlini, *Crit. Care Med.*, 2012, **40**, 544; M. Kubeil, R. R. Vernooij, C. Kubeil, B. R. Wood, B. Graham, H. Stephan, and L. Spiccia, *Inorg. Chem.* 2017, ***56*** **(10)**, 5941.
[21] R. Tatikonda, and M. Haukka, *Acta Cryst.* 2017, **E73**, 556; D. H. Gibson, B. A. Sleadd, M. S. Mashuta, and J. F. Richardson, *Organometallics* 1997, **16**, 4421.
[22] G. B. Deacon, J. M. Patrick, B. W. Skelton, N. C. Thomas and A. H. White, *Aut. J. Chem.*, 1984, **37**, 929.
[23] H. Tabe, K. Fujita, S. Abe, M. Tsujimoto, T. Kuchimaru, S. Kizaka-Kondoh, M. Takano, S. Kitagawa, and T. Ueno, *Inorg. Chem.* 2015, **54**, 215.
[24] T. Santos-Silva, A. Mukhopadhyay, J. D. Seixas, G. J. Bernardes, C. C. Romão, and M. J. Romão, *J. Am. Chem. Soc*. 2011, **133**, 1192.
[25] M. F. Santos, J. D. Seixas, A. C. Coelho, A. Mukhopadhyay, P. M. Reis, M. J. Romão, C. C. Romão, and T. Santos-Silva, *J. Inorg. Biochem.* 2012, **117**, 285.
[26] G. Tamasi, A. Carpini, D. Valensin, L. Messori, A. Pratesi, F. Scaletti, M. Jakupec, B. Keppler, and R. Cini, *Polyhedron* 2014, **81**, 227.
[27] A. Merlino, *Coord. Chem. Rev.* 2016, **326**, 111.
[28] E. C. Constable, E. L. Dunphy, C. E. Housecroft, M. Neuburger, S. Schaffner, F. Schaper and S. R. Batten, *Dalton Trans.* 2007, 4323.
[29] J. Compain, M. Stanbury, M. Trejo, and S. Chardon-Noblat, *Eur. J. Inorg. Chem.* 2015, 5757.
[30] A. M. Mansour, *Polyhedron* 2014, **78**, 10.
[31] T. Yanai, D. Tew, and N. Handy, *Chem. Phys. Lett.* 2004, **393**, 51; F. Weigend and R. Ahlrichs, *Phys. Chem. Chem. Phys.*, 2005, **7**, 3297.
[32] D. Nguyen, and C. Boyer, *ACS Biomater. Sci. Eng.* 2015, **1(10)**, 895; S. Mclen, B. E. Mann, and R. K. Poole, *Anal. Biochem.* 2012, **427**, 36.
[33] S. Mahadevan and M. Palaniandaver, *Inorg. Chem.* 1998, **37**, 693.
[34] A. M. Mansour and O. R. Shehab, *Dalton Trans.* 2018, **47**, 3459.

ACCEPTED MANUSCRIPT

[35] M. Chaves-Ferreira, I. S. Albuquerque, D. Matak-Vinkovic, A. C. Coelho, S. M. Carvalho, L. M. Saraiva, C. C. Romão, G. J. L. Bernardes, *Angew.Chem. Int. Ed.* 2015, **54**, 1172; *Angew. Chem.* 2015, **127**, 1188; H. Tabe, K. Fujita, S. Abe, M. Tsujimoto, T. Kuchimaru, S. Kizaka-Kondoh, M. Takano, S. Kitagawa, T. Ueno, *Inorg. Chem.* 2015, **54**, 215; F. Zobi, B. Spingler, *Inorg. Chem.* 2012, **51**, 1210. G. Tamasi, A. Merlino, F. Scaletti, P. Heffeter, A. A. Legin, M. A. Jakupec, W. Berger, L. Messori, B. K. Keppler and R. Cini, *Dalton Trans.*, 2017, **46**, 3025.

[36] N. Pontillo, G. Ferraro, L. Messori, G. Tamasi, A. Merlino, *Dalton Trans.* 2017, **46**, 9621.

[37] A. Maroń, A. Szlapa, T. Klemens, S. Kula, B. Machura, S. Krompiec, J. Malecki, A. Świtlicka-Olszewska, K. Erfurt and A. Chrobok, *Org. Biomol. Chem.* 2016, **14**, 3793.

[38] A. D. Becke, *J. Chem. Phys*. 1993, ***98***, 5648.

[39] P. J. Hay and W. R. Wadt, *J. Chem. Phys.* 1985, **82**, 270; *J. Chem. Phys.* 19852, **82**, 284.

[40] T. Yanai, D.P. Tew, and N.C. Handy, Chem. Phys. Lett. 2004, **393**, 51.

[41] M. J. Frisch, G. W. Trucks, H. B. Schlegel, G. E. Scuseria, M. A. Robb, J. R. Cheeseman, V. G. Zakrzewski, J. A. Montgomery, R. E. Stratmann, J. C. Burant, S. Dapprich, J. M. Millam, A. D. Daniels, K. N. Kudin, M. C. Strain, O. Farkas, J. Tomasi, V. Barone, M. Cossi, R. Cammi, B. Mennucci, C. Pomelli, C. Adamo, S. Clifford, J. Ochterski, G. A. Petersson, P. Y. Ayala, Q. Cui, K. Morokuma, D. K. Malick, A. D. Rabuck, K. Raghavachari, J. B. Foresman, J. Cioslowski, J. V. Ortiz, A. G. Baboul, B. B. Stefanov, G. Liu, A. Liashenko, P. Piskorz, I. Komaromi, R. Gomperts, R. L. Martin, D. J. Fox, T. Keith, M.A. Al-Laham, C. Y. Peng, A. Nanayakkara, C. Gonzalez, M. Challacombe, P. M. W. Gill, B. G. Johnson, W. Chen, M.W. Wong, J.L. Andres, M. Head-Gordon, E.S. Replogle, J.A. Pople, GAUSSIAN 03 (Revision A.9), Gaussian, Inc., Pittsburgh, 2003.

[42] K. A. Meadows, F. Liu, J. Sou, B. P. Hudson and D. R. McMillin, *Inorg. Chem.* 1993, **32**, 2919.

ACCEPTED MANUSCRIPT

ACCEPTED MANUSCRIPT

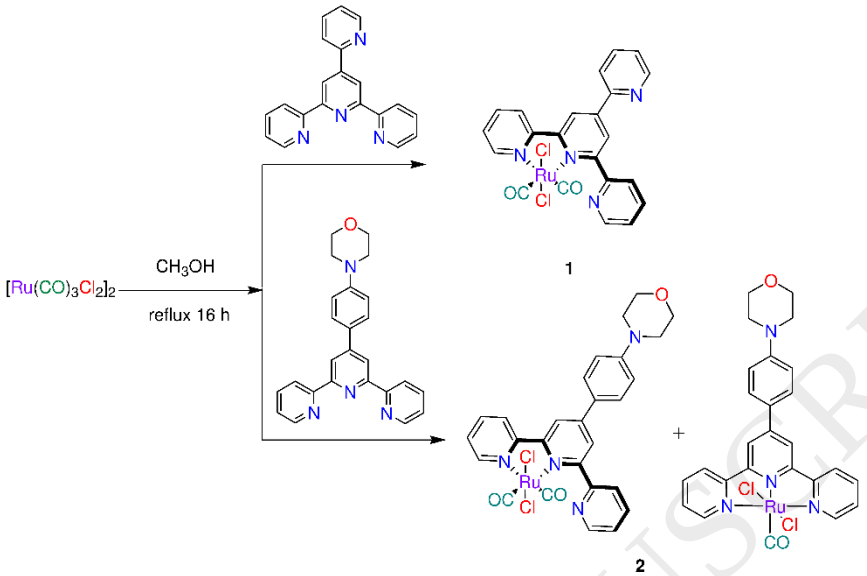

Scheme 1: Synthesis of the {Ru(CO)$_x$}-core terpyridine complexes (L^{PY} (**1**) and L^{morph} (**2**)).

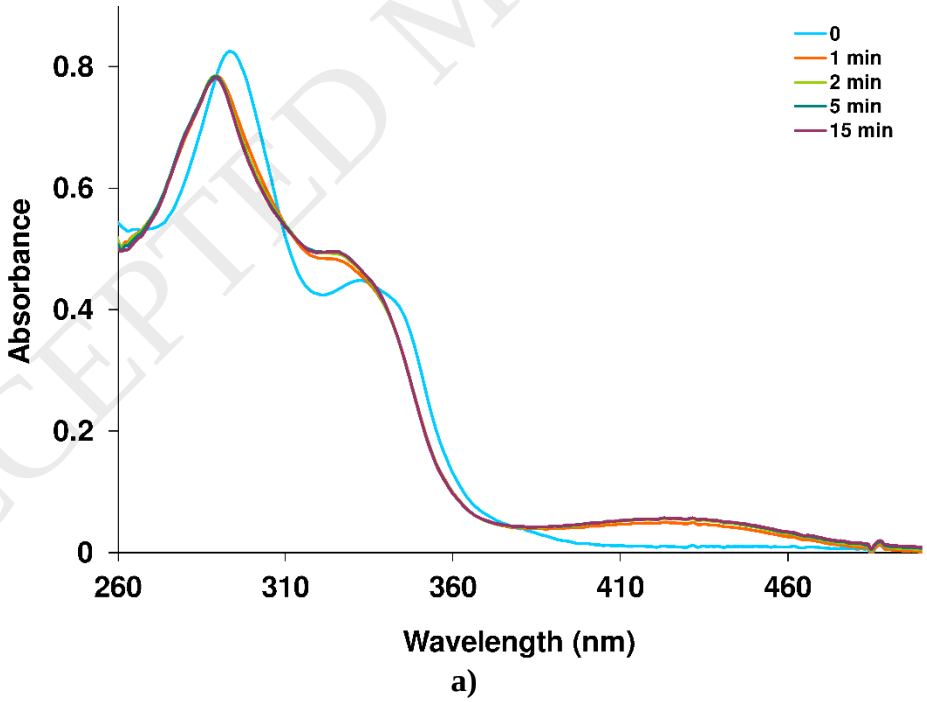

a)

ACCEPTED MANUSCRIPT

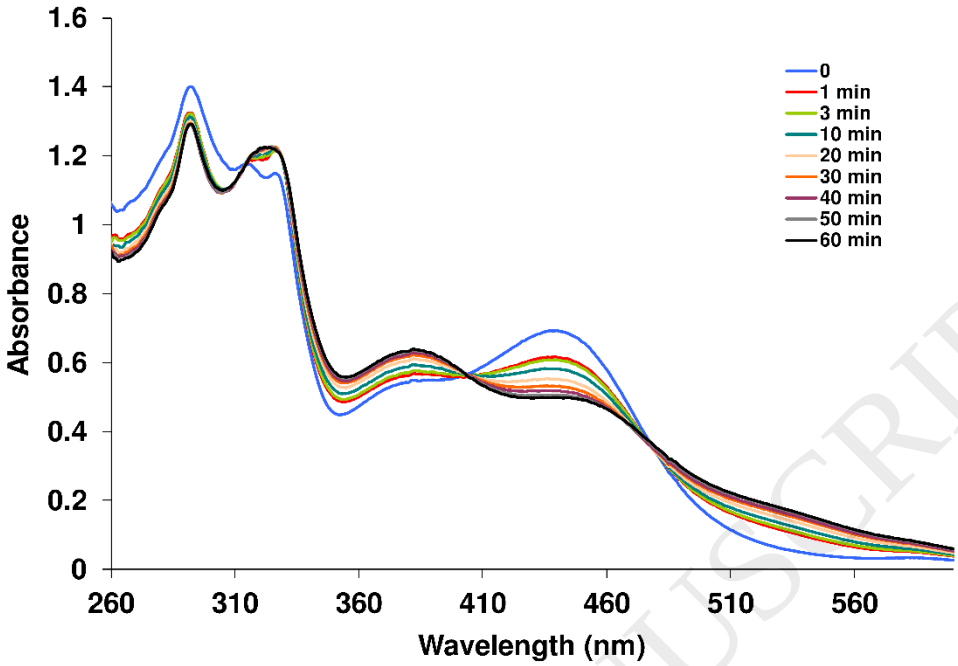

b)

Figure 1. UV/Vis spectral changes of: a) **1**; and b) **2** (in DMSO) upon photolysis at 365 nm (power = 10 mW/cm) for 0–15 and 0–60 min, respectively, after incubation in the dark for 16 h.

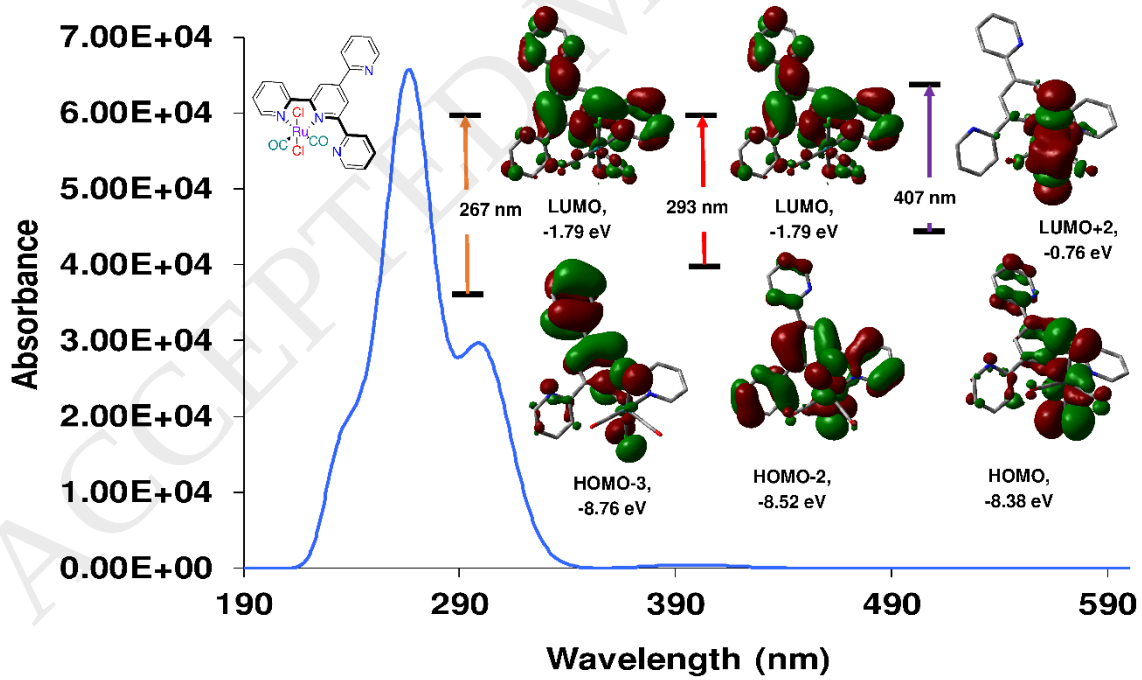

a)

ACCEPTED MANUSCRIPT

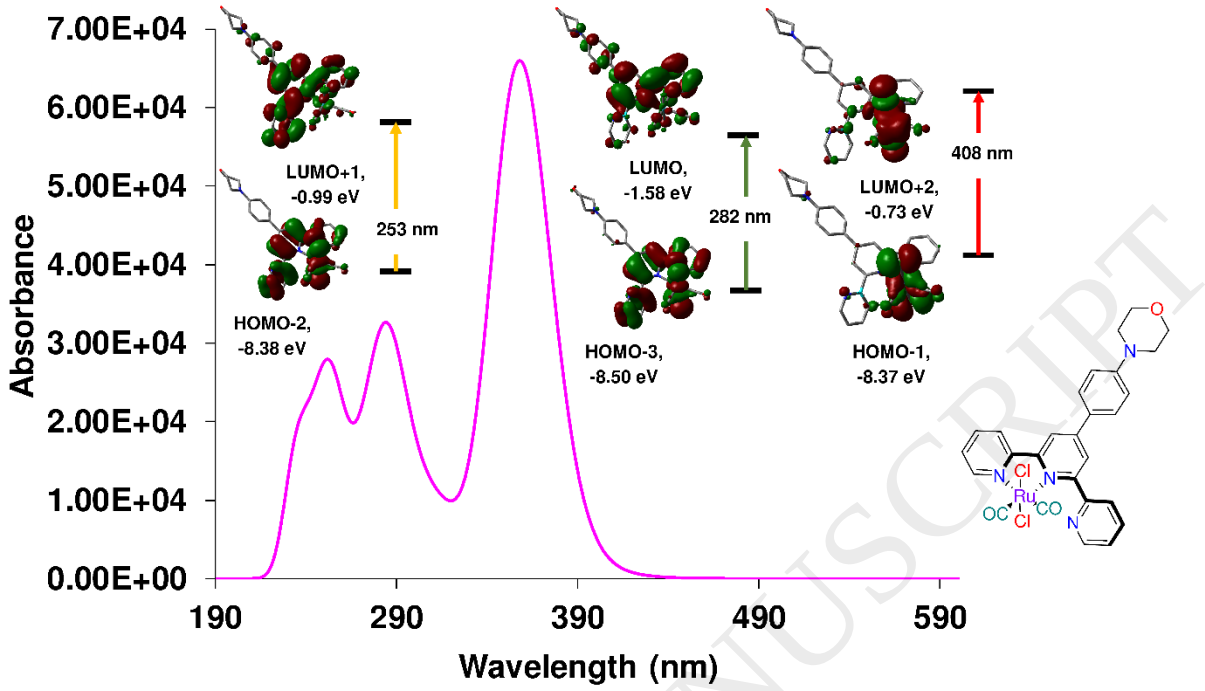

b)

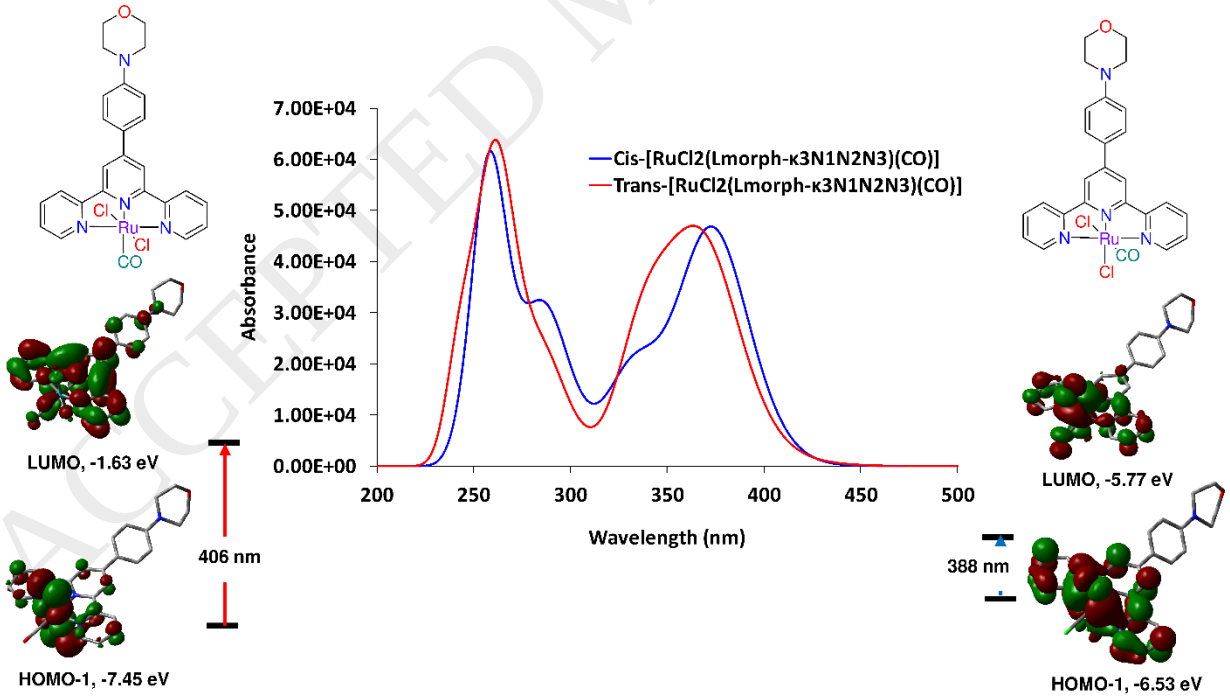

c)

ACCEPTED MANUSCRIPT

Figure 2. Selected frontier molecular orbitals of the ground-state optimized structures of a) **1**, b) *cis*-(CO,CO)-[$RuCl_2(L^{morph}$-$\kappa^2N^1N^2)(CO)_2$] and c) cis- and trans-[$RuCl_2(L^{morph}$-$\kappa^3N^1N^2N^3)(CO)$] calculated at cam-B3LYP/LANL2DZ level of theory, including LANL2DZ ECP.

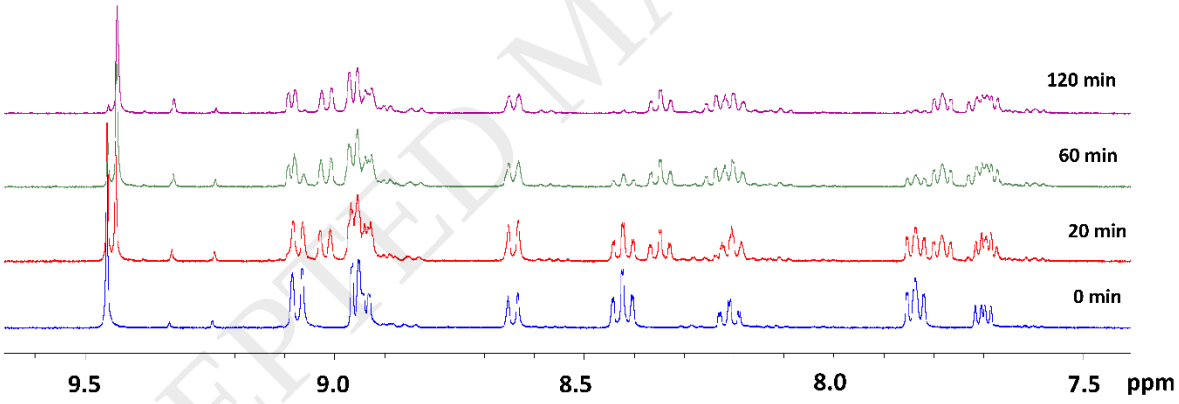

Figure 3. ^{1}H NMR spectral changes of **1** (in [D_6] DMSO) upon the exposure to light source at 365 nm for 120 min.

ACCEPTED MANUSCRIPT

ACCEPTED MANUSCRIPT

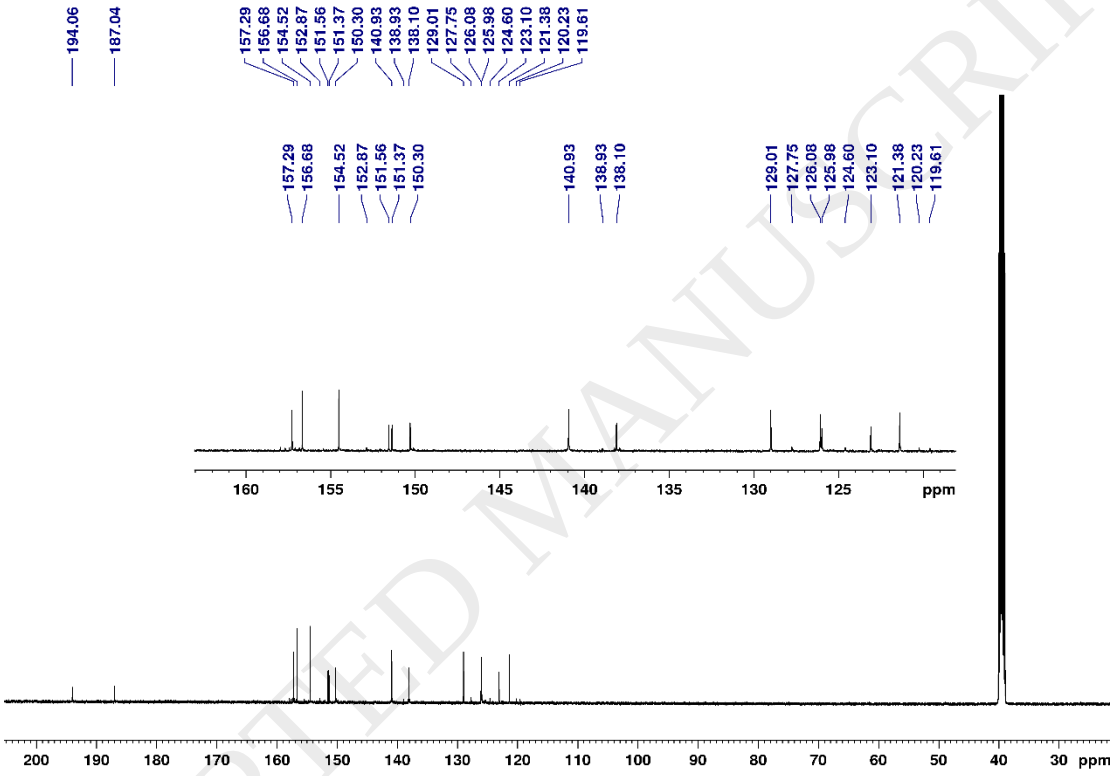

a)

ACCEPTED MANUSCRIPT

ACCEPTED MANUSCRIPT

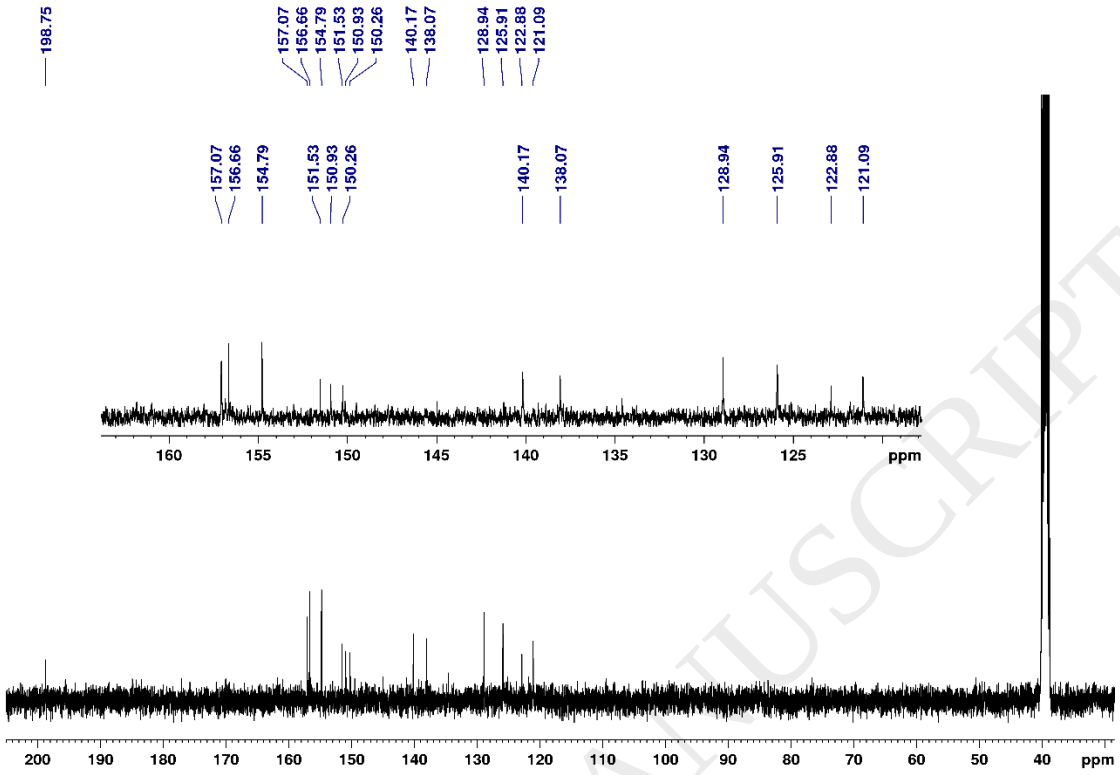

b)

Figure 4. ^{13}C NMR spectra of **1** a) before and b) after exposure to light source for 120 min.

ACCEPTED MANUSCRIPT

ACCEPTED MANUSCRIPT

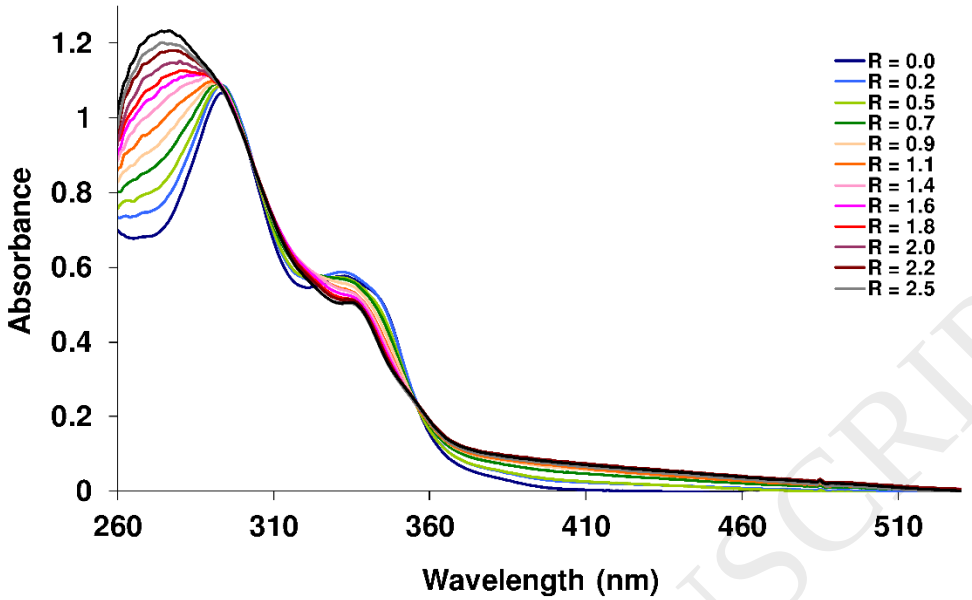

a)

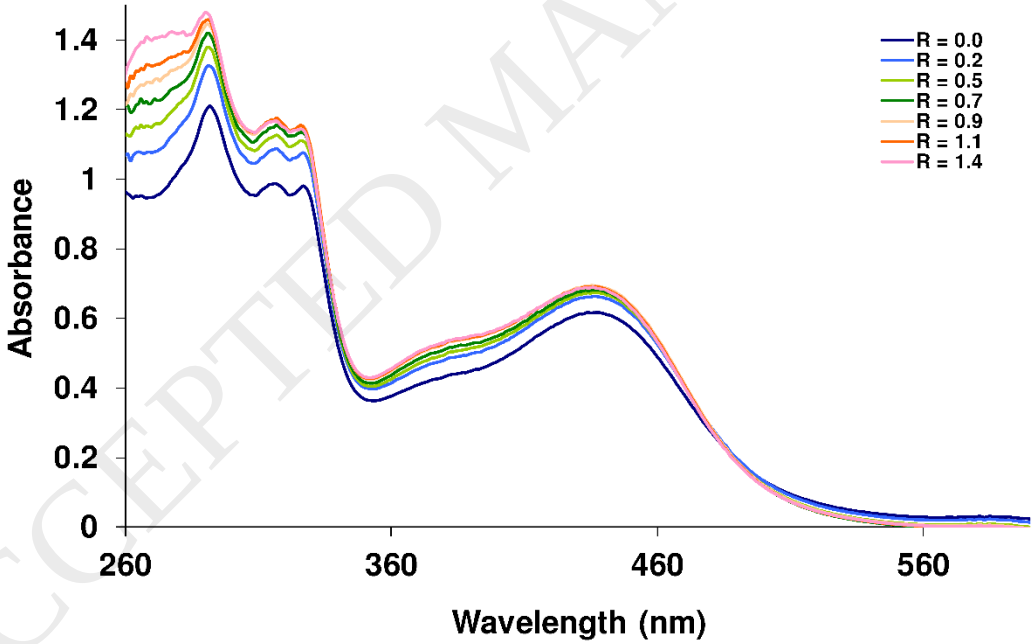

b)

Figure 5. Absorption spectra of complexes a) **1** and d) **2** in Tris-buffer buffer (20% DMSO), in absence (R = 0.0) and presence (R > 0.0) of increasing amounts of CT DNA (R = [DNA]/[complex], [complex] = 1×10^{-5} M)

ACCEPTED MANUSCRIPT

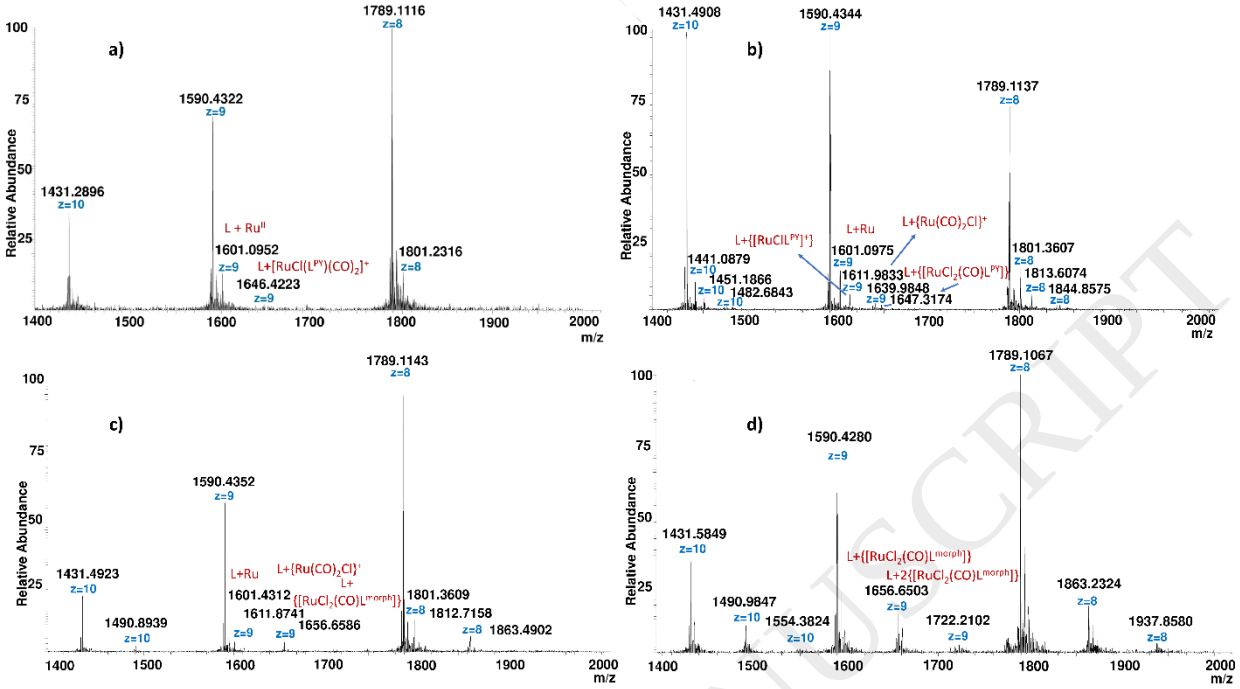

Figure 6. ESI-MS of HEWL-complex adducts a) **1** (in dark), b) **1** (illumination for 20 min.), c) **2** (in dark) and d) **2** (illumination for 20 min.)